

Observations of circumstellar disks with infrared interferometry

Rachel Akeson

Michelson Science Center, Caltech, Pasadena, CA, USA 91125

Abstract

The study of circumstellar disks around young stellar objects is arguably the area of astrophysics on which the technique of infrared interferometry has had the biggest impact. Here I will review the existing set of observations in this field, concentrating on disks but also including jets/winds and stellar properties. At the end, there is a brief discussion of how ongoing technical developments and observational improvements will expand the impact of infrared interferometry on the study of star formation.

Key words: circumstellar disks, infrared interferometry

1 Introduction

The study of circumstellar disks around young stars has been one of the major areas of focus in infrared interferometry observations. One of the most exciting developments in the last few years is the expansion of the interferometers which can contribute to this area of study. As of early 2007, there were over 30 refereed publications describing observations of 66 young stellar objects in the T Tauri, Herbig Ae/Be, FU Ori and high mass young star categories. There are now so many observations that a single review can not mention them all and I will try to give a broad overview starting with the initial observations from several years ago, but also highlighting many of the recent results which show the promise of this observational technique in the next few years. I will attempt to touch on all aspects of YSO observations: disks, jets/winds and stellar properties. Other excellent reviews of this material exist, including Millan-Gabet et al. (2007) in *Protostars and Planets V*.

In this section, I give a brief introduction to star formation to give the context for the observations discussed in the rest of the review. There are many excellent references on this topic; recent reviews from the proceedings of the Protostars and Planet V conference include Beuther et al. (2007) on the formation of massive stars and Klein et al. (2007) on the formation of low mass stars, as well as several chapters separately covering disks, jets and outflows.

The formation paradigm for low and intermediate mass ($<8 M_{\odot}$) has been assembled over many years through the combination of observational and theoretical work. In isolated star formation, which takes place in the nearest molecular clouds such as Taurus and Ophiuchus, a cold clump of gas and dust collapses under self-gravity and forms a central star, still surrounded by its birth cloud. Due to conservation of angular momentum, some of the material collapsing onto the star forms a flattened disk, while other material falls directly onto the star from a surrounding envelope. At this stage, it is commonly accepted that a high velocity jet forms, which ejects only a small mass of material, but serves to rid of the star of much of its initial angular momentum and in the case of energetic outflows, injects energy back into the cloud. After roughly 1 million years (for the case of a $1 M_{\odot}$ star; evolution proceeds more quickly for higher masses) the combination of outflow and in-fall disperses the majority of the envelope and the star is optically revealed. For solar-mass stars, this is the T Tauri phase, while for intermediate masses, these stars are referred to as Herbig Ae/Be stars. A substantial circumstellar disk is still present and many objects at this stage continue to power jets and winds. After several million years (again for a $1 M_{\odot}$ star) the primordial disk is mostly depleted.

The formation of high mass stars is considerably less well understood. A simple scaling of the low and intermediate mass scenario runs into the problem of radiation pressure from the massive protostar halting the accretion before enough material has accumulated to match the most massive stars in the galaxy. There are two primary approaches to overcoming this difficulty. The first is for the accretion to continue through modifications of the collapse scenario, including accretion through a disk, higher accretion rates and radiatively driven instabilities. The second scenario involves a completely different paradigm in which the most massive stars are formed through mergers of lower mass stars or formation in clusters so dense that the accretion rate depends on the total cluster mass. High mass stars can still be embedded and accreting after joining the main sequence. Hypercompact and ultracompact HII region stages, where the massive star is surrounded by a shell of ionized gas, follow the protostellar phase and massive YSOs drive jets and outflows as well.

1.2 Interferometers

There are many current and recently operating optical and infrared interferometers (see reviews in the SPIE Proceedings vol. 6268, *Advances in Stellar Interferometry*). The results discussed here have come from the Palomar Testbed Interferometer (PTI), the Infrared Optical Telescope Array (IOTA), the Keck Interferometer (KI), the Very Large Telescope Interferometer (VLTI) and the Center for High Angular Resolution Astronomy (CHARA) array. The currently operating baseline lengths, wavelengths and website for more information on each of these arrays is given in Table 1.

1.3 Why infrared interferometry?

As outlined in section 1.1, the formation of low and intermediate mass stars involves a clump of gas and dust collapsing under the force of gravity to form a central star, a surrounding envelope, a flattened disk and outflowing material in a jet or wind. All of these components are not observable at every stage due to the high extinction of the envelope and surrounding cloud in the early stages and the low flux levels in the later stages. The star and disk are not observable in the optical and infrared until the T Tauri or Herbig Ae/Be phase when most or all envelope has been accreted or dispersed and it is this stage that most of the infrared interferometry observations are concentrated. For high mass young stars most of the initial envelope must have dispersed before the young star can be observed at these wavelengths.

Infrared interferometry is well matched to the size scales and material temperatures in circumstellar disks. The nearest regions of ongoing star formation are 140 parsecs away. At this distance, 1 AU subtends an angle of 7 milliarcseconds (mas). The fringe spacing (defined here as wavelength/baseline) for a 100 meter baseline is 4 mas at 2 microns and 20 mas at 10 microns. The fringe spacing is an indication of the largest diameter easily detectable on that baseline, as an object with a uniform disk angular diameter equal to the fringe spacing will have a visibility amplitude of 0.2 and a squared visibility amplitude of 0.04. The smallest angular size which can be measured is determined by the measurement precision in establishing the significance of a visibility to be slightly less than one. For an measurement uncertainty of 2% in visibility amplitude squared, a source with an angular diameter 1/8 of the fringe spacing is detected as resolved at the 3σ level, i.e. 0.5 mas for a 100 meter baseline at 2 microns. Higher precision measurements are discussed in more detail in section 7.2.

Near-infrared wavelengths (H and K, 1.6 and 2.2 microns respectively) are

Table 1

The current operational capabilities of infrared interferometers discussed in this review.

Array name	Palomar Testbed Interferometer (PTI)
Baseline range (m)	85-110
Aperture diameter (m)	0.4
Wavelength bands	H,K
URL	http://msc.caltech.edu/missions/palomar/
Array name	Infrared Optical Telescope Array (IOTA)
Baseline range (m)	15-40
Aperture diameter (m)	0.4
Wavelength bands	H,K
URL	http://tdc-www.harvard.edu/IOTA/
Array name	Keck Interferometer (KI)
Baseline range (m)	85
Aperture diameter (m)	10
Wavelength bands	H,K,N
URL	http://planetquest.jpl.nasa.gov/keck
Array name	Very Large Telescope Interferometer (VLTI)
Baseline range (m)	47-130/8-200
Aperture diameter (m)	8/1.8
Wavelength bands	J,H,K,N
URL	http://www.eso.org/projects/vlti/
Array name	Center for High Angular Resolution Astronomy (CHARA)
Baseline range (m)	30-330
Aperture diameter (m)	1
Wavelength bands	H,K
URL	http://www.chara.gsu.edu/CHARA/array.html

primarily sensitive to material emitting near 1000 K, which corresponds to material in the inner disk, while mid-infrared observations (N band, 10 microns) are most sensitive to material at hundreds of Kelvin, corresponding to the middle disk and the habitable zone. Infrared interferometry observations are complimentary to observations at other wavelengths, particularly millimeter interferometry which probes the entire disk mass on scales from tens to

hundreds of AU.

The current infrared arrays generally collect data on one or a few simultaneous baselines with no or limited phase information (also see section 7 for recent closure phase developments and prospects), thus no images have been constructed using long-baseline interferometry data of a YSO. However, these data can still provide significant and unique constraints on the structures in disks. The general method for observing disks is:

- (1) Get visibility measurements on your favorite target.
- (2) Determine the contribution from all components in the system. At current resolutions, the central star is unresolved. Scattered light or thermal emission from an extended envelope will generally be incoherent and will contribute to the total flux. This extended component is often limited by the field-of-view, particularly for the large aperture arrays. This flux determination can be done by spectral energy distribution (SED) fitting or high resolution spectroscopy veiling measurements.
- (3) Fit your favorite model to the remaining (hopefully resolved) emission component. If there is sufficient baseline coverage, the inclination angle can be fit, but often this must be assumed from other measurements. All emission components from step 2 must be accounted for in the visibility calculations.

$$V_{total} = \frac{V_{star}f_{star} + V_{disk}f_{disk} + V_{extended}f_{extended}}{f_{star} + f_{disk} + f_{extended}}$$

$$\approx \frac{V_{star}f_{star} + V_{disk}f_{disk}}{f_{star} + f_{disk} + f_{extended}}$$

Models fit to the disk visibility range from geometric (uniform disk, Gaussian, ring) which are useful for establishing the size scales and for comparison among samples of sources to full radiative transfer with many kinds of input data. In this procedure it is also crucial to reliably establish the model uncertainties which are determined by both the measurement uncertainties and the uncertainties in step 2. Many T Tauri stars are variable in the near-infrared and so the uncertainties from step 2 can often dominate the physical parameter uncertainties.

2 Circumstellar disks

Circumstellar disks around young stars are made up of several regions and the wavelengths and techniques used to observe these regions vary with the characteristic temperatures and size scales involved. In infrared interferometry,

the near-infrared is used for the inner edge of the gas and dust disk, while the mid-infrared studies extended from the inner edge to several AU into the disk.

2.1 Inner disk: dust and gas

The questions to address using infrared interferometry in the inner disk include:

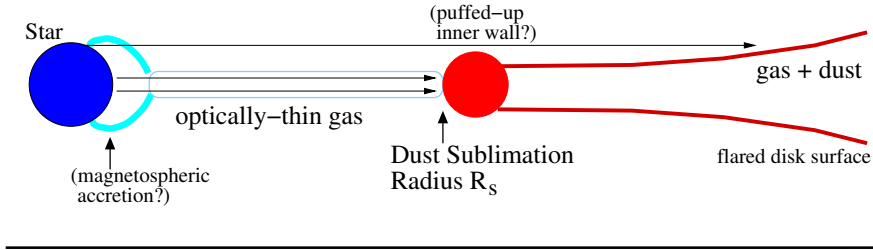
- What is the spatial distribution of gas and dust in the inner disk?
- Is there emission from another component on small scales?

The overall model in which most of these observations take place includes the central star, which for Herbig and T Tauri stars is a few solar radii and therefore unresolved, and the resolved disk whose visibility will depend on the size and flux profile. These disks often extend to >100 AU, but only the central few AU are warm enough to have significant emission at near-infrared wavelengths.

Classical models of geometrically flat accretion disks contain optically thick material all the way into the magnetospheric radius where the star's magnetic field lines truncate the disk. The disk is composed of gas and dust, except in the central region where the temperature is so high (> 1500 K) that the dust sublimates. In this model, the predicted near-infrared visibility is very high as the magnetospheric radius is a few times the stellar radius (Figure 1). However, the initial observations with PTI and IOTA did not follow the predictions for T Tauri and Herbig stars. A survey of 15 Herbig stars by Millan-Gabet et al. (2001) found the resolved sources to be larger than predicted from an accretion disk with $T \propto r^{-3/4}$ and no asymmetries observed on short to medium baselines. The first observations of T Tauri stars by Akeson et al. (2000) found that disk emission from T Tau N and SU Aur came from radii larger than predicted from SED models. Interestingly, the very first YSO observed was FU Ori itself, which did match the predicted structure (more on FU Ori in section 4).

At the same time, other techniques such as aperture masking were used to study even more massive YSOs. In the images of LkH α 101 of Tuthill et al. (2002) the disk emission is in an asymmetrically bright ring which the authors find to be consistent with the size expected for the sublimation point of optically thin dust. Several groups of modelers (Natta et al., 2001; Dullemond et al., 2001; Muzerolle et al., 2003) proposed a solution to these observations and to the excess emission seen in the near-infrared SEDs of Herbig objects. In their physical models the central gas-only region is optically thin and therefore the dust sees the stellar flux directly. This direct heating results in the inner edge being vertically extended (Figure 1). These models can produce both the

Direct heating of inner dust disk



"Standard" Disk Model – oblique disk heating

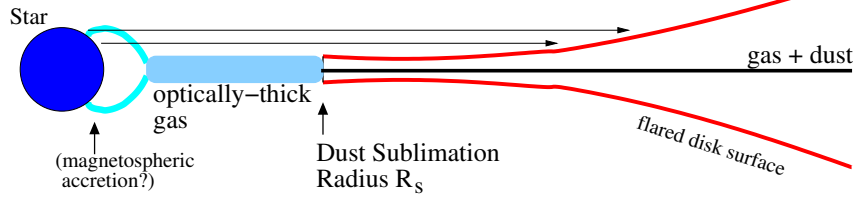


Fig. 1. A schematic representation of the two models with optically thin material within the dust sublimation radius (top) and optically thick material to the magnetospheric radius (bottom). Figure taken from Millan-Gabet et al. (2007).

near-infrared bump seen in the SEDs of Herbig stars, as the vertically extended inner rim has a larger emission region, and the resolved visibilities, as the near-infrared emission from the disk is dominated by inner rim, which is far enough from the central star to be resolved by interferometers with baselines of tens to a hundred meters.

More observations from other groups (Eisner et al., 2004; Monnier et al., 2005; Akeson et al., 2005a) mostly using KI significantly expanded the sample of observed T Tauri and Herbig objects. Observations with longer baselines revealed the asymmetries expected for inclined disks (Eisner et al., 2004; Akeson et al., 2005b) but the overall trend of size corresponding to the dust sublimation radius held for the Herbig Be and T Tauri stars. However, the Herbig Ae stars seem consistent with the older geometrically thin but optically thick models (Figure 2). This difference could arise from a fundamental difference in the formation process of these higher mass stars or could simply be due to the different evolutionary state they are in when they become optically visible.

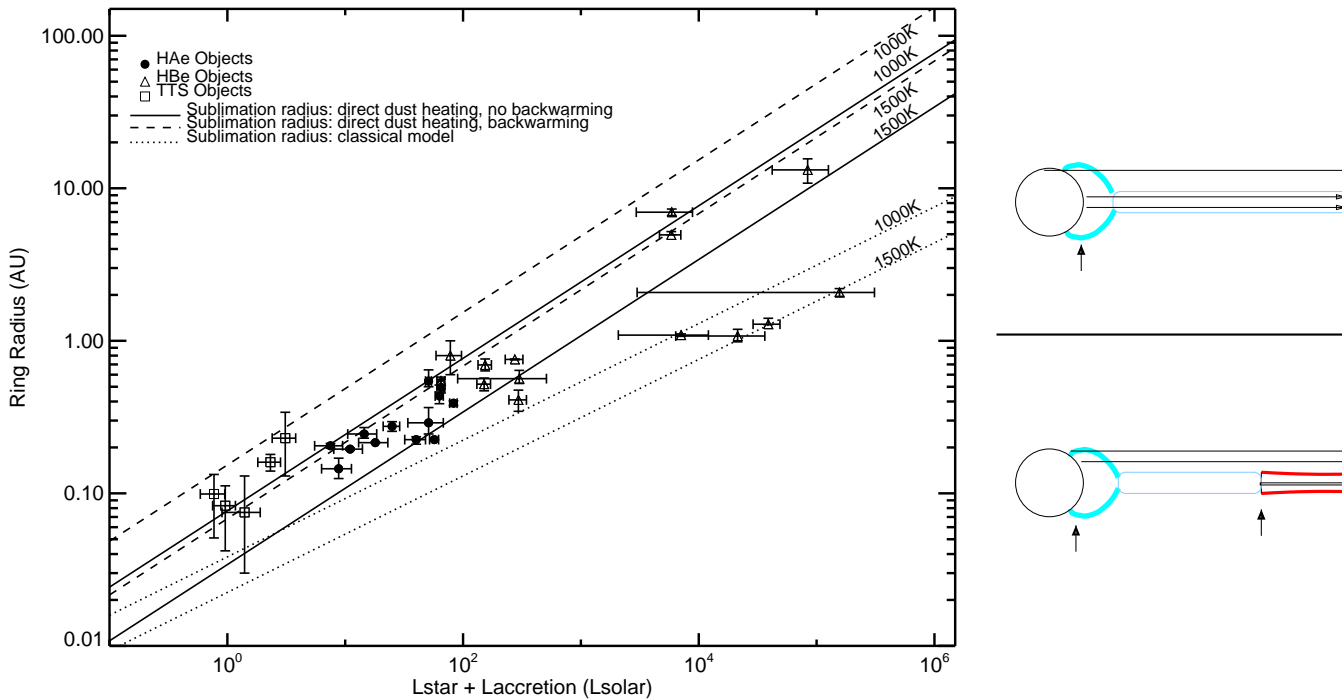


Fig. 2. The measured sizes of Herbig Ae/Be and T Tauri stars vs the total stellar and accretion luminosity are plotted against sublimation radii for directly heated dust (solid and dashed lines) and for oblique heating (dotted line). Figure taken from Millan-Gabet et al. (2007).

The early studies all used continuum observations which are dominated by dust emission in the low to intermediate mass sources. Using higher spectral resolution ($R >$ several hundred) it is possible to measure the visibility across spectral features in the near-infrared and directly compare the physical size of the gas-only region (line emission) to the gas and dust (continuum emission) region. Relevant lines in the near-infrared include H_2O , CO and hydrogen $\text{Br}\gamma$. Tatulli et al (in prep) used the AMBER instrument on the VLTI to observe the high mass YSO 51 Oph at high spectral resolution in the K band. They detected flux and closure phase (see section 7.4) across the CO bandhead lines which are consistent with Keplerian rotation in the central portion of the disk. Another example of the power of spectrally resolved observations is shown in Figure 3. Tatulli et al. (2007) measured the visibility across the $\text{Br}\gamma$ line for the Herbig Ae star HD 104237. The visibility did not change from the continuum value and, given the line flux (not shown here) this is most consistent with the $\text{Br}\gamma$ originating in an outflowing wind rather than in the disk.

Observations have also been extended to somewhat older T Tauri stars, such as TW Hya, which has an estimated age of 10 Myr and is located 55 pc away. Eisner et al. (2006) made K band observations with KI and found the source to be resolved with a high visibility. Jointly modelling the SED and the visibility,

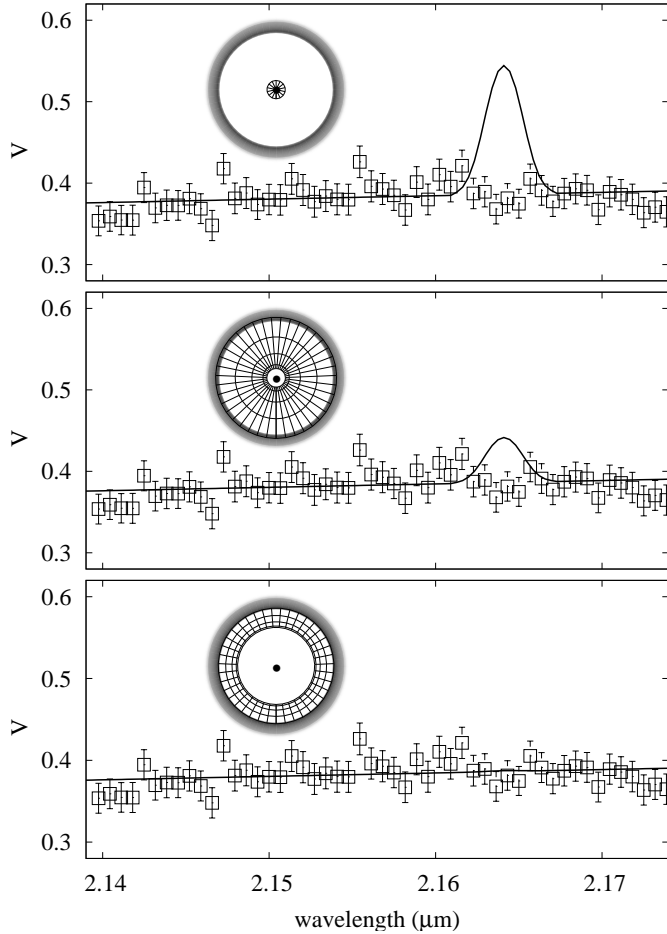


Fig. 3. Comparison between the observed visibilities (empty square with error bars) and the predictions (solid curves) of the simple geometrical models for the $\text{Br}\gamma$ emission (sketched in the same panels) from HD 104237. The observed visibilities are scaled to match the continuum value predicted by a "puffed-up" inner rim model. The continuum emission arises both from the stellar photosphere ($\approx 20\%$) and from the dusty disk inner rim, located at the dust evaporation distance $R_{\text{rim}} = 0.45$ AU and which appears as the bright gray scale ring. The $\text{Br}\gamma$ emission regions are shown as grid surfaces. The three panels illustrate three possible origins from the $\text{Br}\gamma$ emission: the upper panel represents the magnetospheric accretion model in which the $\text{Br}\gamma$ emission originates very close to the star, inside the corotational radius $R_{\text{corot}} = 0.07$ AU; in the middle panel the $\text{Br}\gamma$ emission originates between R_{corot} and the rim radius $R_{\text{rim}} = 0.45$ AU, representing the gas within the disk model; the bottom panel shows the outflowing wind model, in which the emission is confined close to the inner rim, between ~ 0.2 AU and ~ 0.5 AU. Figure and text from Tatulli et al. (2007)

they found that large grains (those with a wavelength opacity dependance of $\beta=0$) can not fit the visibility data, while smaller grains ($\beta = 1$) can, although both model grains match the SED. These grains extend to within 0.06 AU of the central star and as small grains have a lifetime much smaller than the age of the system due to radiation pressure, these grains must be replenished by

some mechanism.

2.2 Middle disk: composition and structure

The middle disk (here roughly defined as 1 to tens of AU) has temperatures of several hundred Kelvin and is well probed by observations at mid-infrared wavelengths. Interferometry observations on 100 meter baselines will resolve structures on 1 AU scales at the distance to the nearest star formation regions ($d \sim 150$ pc), but the more massive objects, particularly the Herbig Be stars are at much larger distances and the corresponding spatial resolution is lower.

The majority of mid-infrared observations have been of Herbig Ae/Be stars with the MIDI instrument at VLTI. Figure 4 shows the measured half light radius in AU plotted against the mid-infrared color from a sample of objects observed by Leinert et al. (2004). The most red object in mid-infrared colors (HD 100456) has a larger spatial radius than most of the more blue objects. These results are roughly consistent with the classification scheme proposed by Meeus et al. (2001) of Group I flared disks, which appear larger and more red in the mid-infrared and Group II sources, which are self-shadowed and have a flatter geometric profile (see graphic at bottom of Figure 4). Leinert et al. (2004) also find qualitative agreement between their results and the predictions of the disk models for these objects of Dominik et al. (2003) which were fit only to the SEDs.

However, as more data are collected on a larger sample of sources and as some sources are considered in detail, exceptions to this classification scheme have been found. For example, Preibisch et al. (2006) obtained MIDI/VLTI data on the Herbig A star HD 5999 and found visibilities much higher than those in the Leinert et al. (2004) sample. In their models, the measured visibilities correspond to a physical size of 1 to 3 AU and if the disk has a power-law density distribution, it must be truncated at 2–3 AU in order to match the high visibility.

In addition to measuring the physical scales of the disk emission, the mid-infrared visibilities are generally spectrally dispersed with enough resolution to probe the composition of the disk as a function of radius. The mid-infrared region contains silicate features at ~ 10 microns, and so is ideal for studying the mineralogy. Figure 5 shows an excellent example of this technique toward three different stars. The left-hand spectra give the correlated flux as a function of baseline for baselines which probe the inner disk (i.e. long baselines sensitive to emission from radii of 1–2 AU) while the right-hand spectra show the flux for the total disk as probed in the mid-infrared (radii from 1–20 AU).

The mineralogy studies generally show that the inner 2 AU of these disks have

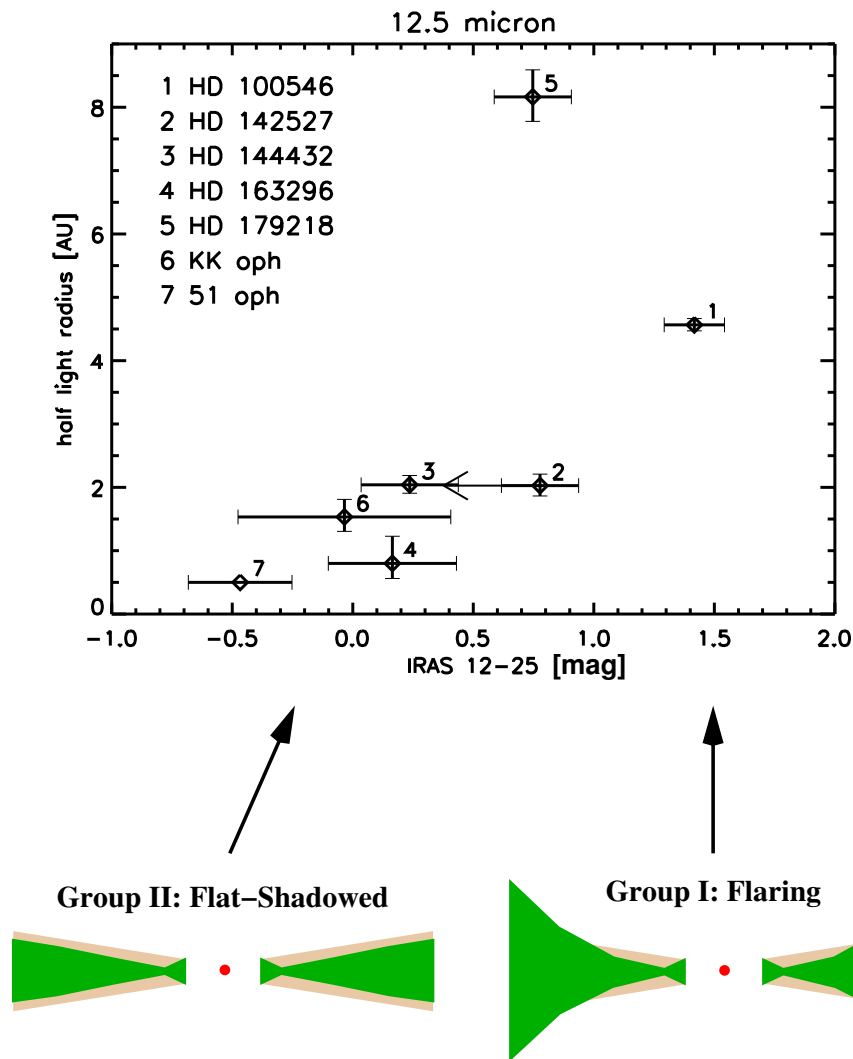


Fig. 4. The relationship between the measured mid-infrared size and the infrared slope as measured from IRAS colors for a sample of Herbig stars observed with MIDI on the VLTI. The size-color relation is consistent with the SED classification of Meeus et al. (2001). Figure taken from Millan-Gabet et al. (2007).

larger silicate grains and a higher fraction of silicates in crystalline structures (40-100%) as compared to the outer regions. This is consistent with chemical equilibrium processing and thermal annealing in the inner disk which is predicted by some models which include radial mixing (see e.g. Gail, 2004; Bockelée-Morvan et al., 2002). Although there are differences in the details of the spectra for individual objects, the similarities are striking given the range of stellar properties. In Figure 5 the stellar luminosity ranges from $0.3 L_{\odot}$ for TW Hya to $10 L_{\odot}$ for HD 144432 and $18 L_{\odot}$ for RY Tau.

With the expansion of the lists of observed YSOs, there are now several objects with observations from the near-infrared to the mid-infrared and some studies have begun modelling these more complete data sets which span from the inner

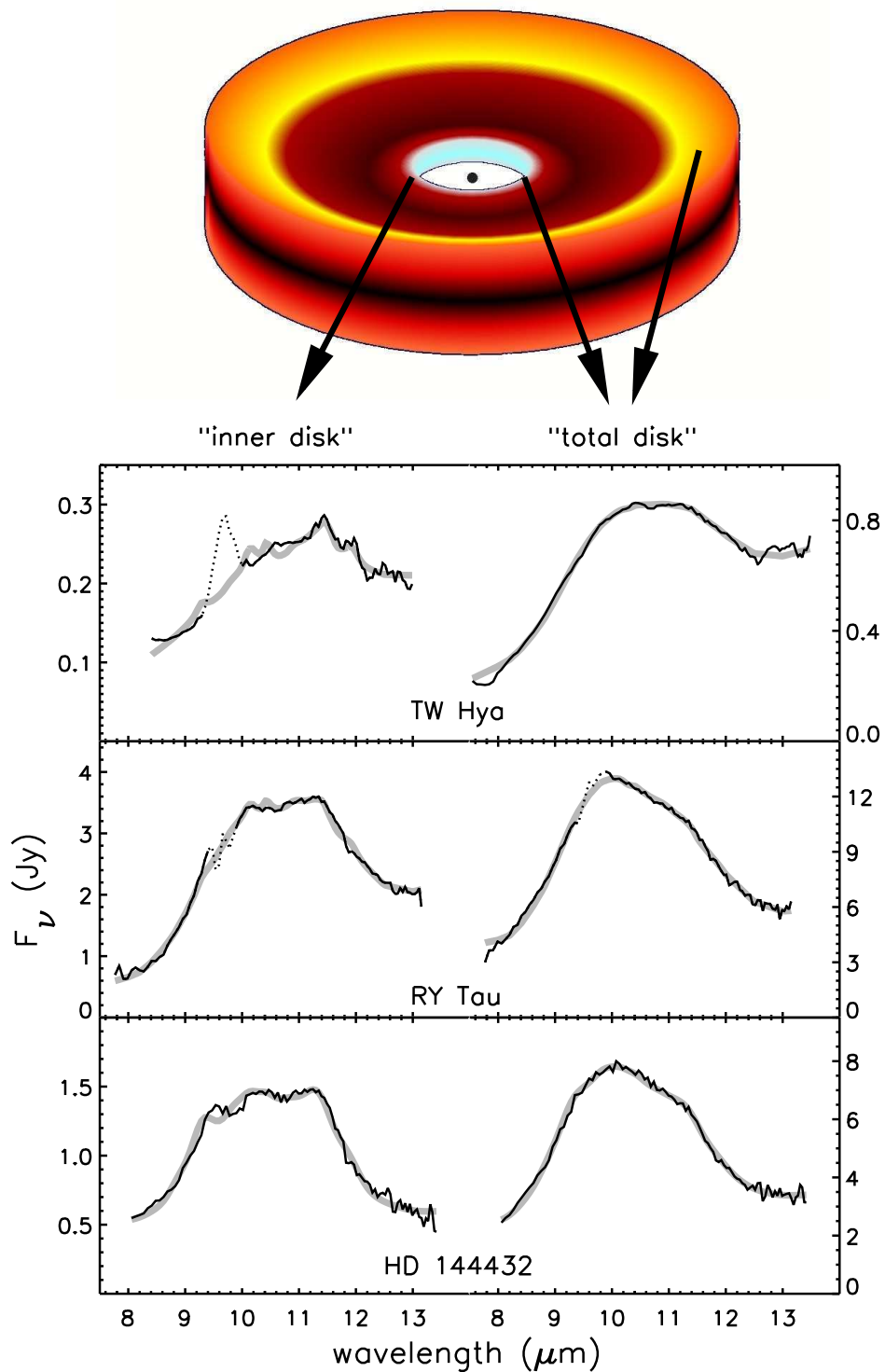


Fig. 5. The infrared spectra of young stellar objects as a function of radius showing evidence for radial changes in the dust composition. The spectra on the left are for the inner 1-2 AU, while those on the right are for the total disk emitting in the mid-infrared. Figure provided by R. van Boekel and taken from Millan-Gabet et al. (2007).

disk edge to tens of AU. One example is the Herbig Be star MWC 147, for which Kraus et al (in prep) have combined data from H(IOTA), K(AMBER/VLTI) and N (MIDI/VLTI) bands. If a disk model with a temperature profile of $T \propto r^{-3/4}$ is fit to the K band, the predicted mid-infrared diameter is much smaller than the measured mid-infrared diameter and in fact, this model does not fit well even within the K band. Kraus et al. have performed two dimensional radiative transfer modelling and can reproduce the data with an optically thick gaseous disk inside of the dust sublimation radius.

2.3 Disk summary

Overall, the infrared interferometric observations of circumstellar disks show strong support for the inner dust radius being located at the dust sublimation radius and this has been shown to apply at luminosities from 1 to $\sim 10^4 L_{\odot}$. At even higher luminosities, the disk emission is consistent with a optically thick disk extending to the magnetospheric radius. The mid-infrared observations follow the classification of Herbig Ae/Be sources into flared and self-shadowed morphologies and higher spectral resolution is tracing the dust composition as a function of radius. However, as observational capabilities improve in sensitivity and precision, even these new models are being challenged and some of the new questions being addressed are discussed in section 7.

3 Jet and winds

Increases in sensitivity and spectral resolution are allowing teams to investigate the jet and wind components of young stellar objects, which are thought to be a ubiquitous component of star formation. In the first high resolution near-infrared observations, Malbet et al. (2007) observed the disk and Br γ emission from massive young star MWC 297. The Br γ emission clearly has a lower visibility than the continuum from the disk (Figure 6) and Malbet et al. (2007) have modelled this object with an optically thick disk and a stellar wind with a latitude-dependant stellar wind outflow above the disk surface.

4 FU Oris

FU Ori's are a sub-class of T Tauri stars which undergo major brightening events (see review by Hartmann & Kenyon, 1996). This brightening is ascribed to a large increase in the disk accretion rate. The SEDs are consistent with emission arising from accretion luminosity alone (no stellar component) and

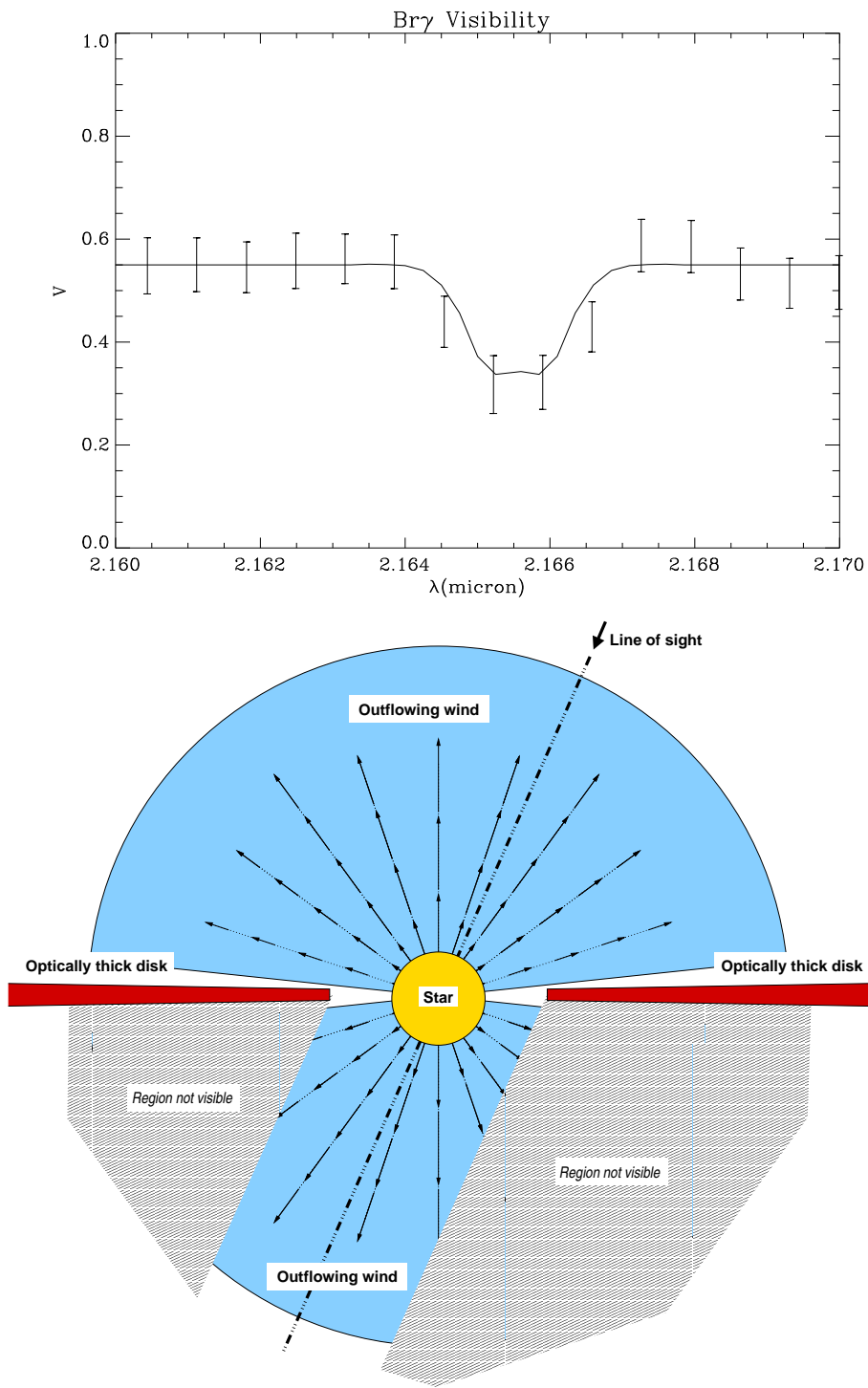


Fig. 6. Top) The visibility observed with AMBER (points with error bars) and the one obtained from the outflowing wind model (full line) for MWC 297. Bottom) Sketch of the model including an optically thick disk and an outflowing wind (edge-on view). The receding part of the wind is only partly visible because of the screen made by the optically thick disk. Figure from Malbet et al. (2007).

accretion rates up to $10^{-4} M_{\odot}/\text{year}$ are derived. Thus the SED is in some ways simpler to interpret than for other disk sources and if it is truly accretion dominated will follow a temperature profile of $T \propto r^{-3/4}$. The disk extends all the way to the stellar surface, therefore a simple model can be constructed which has only 1 parameter, the temperature scaling. Thus, FU Ori sources are ideal for studying accretion disks.

FU Ori itself was the first YSO observed with infrared interferometry and the observations at PTI by Malbet et al. (1998) were consistent with the predictions of the accretion dominated model. A more recent compilation of data by Malbet et al. (2005) from PTI, IOTA and VLTI, at H and K and over a range of baselines makes this the best studied YSO to date. The more detailed study confirmed that the data are consistent with a young star undergoing massive accretion and they could constrain not only the accretion rate, but also the disk inclination and position angle. Figure 7 shows this model fit to the SED and the visibilities.

However, measurements of some of the few other members of this class observable with infrared interferometers revealed that this simple accretion disk prescription does not work on all sources. Millan-Gabet et al. (2006a) observed 3 more FU Oris and found that the single parameter model when fit to the SED, overestimated the observed visibility (Figure 8). These visibilities could be matched by including emission larger scales, such as scattering from an extended envelope.

FU Ori's have also now been observed in the mid-infrared. Abraham et al. (2006) observed V1647 Ori which has undergone a recent outburst and may be an FU Ori or a member of a related class called UX Or objects. They found no spectral features in the mid-infrared, which suggests large dust grains and a temperature profile of $T \propto r^{-0.53}$, more shallow than the canonical accretion profile. FU Ori itself was also observed in the mid-infrared by Quanz et al. (2006) who found a weak and broad silicate feature consistent with large grains. They also found a break in the temperature profile with $T \propto r^{-0.75}$ at radii less than 3 AU and $T \propto r^{-0.52}$ at radii larger than 3 AU. The large grains implied by both these results place strong constraints on dust evolution models as most scenarios require FU Ori objects to be very young.

5 Stellar properties

A standard use of optical interferometers is the determination of binary physical orbits and stellar properties. The advent of large aperture interferometers has allowed this to extend to young stellar objects. This is particularly important for star formation models as there are few mass and luminosity deter-

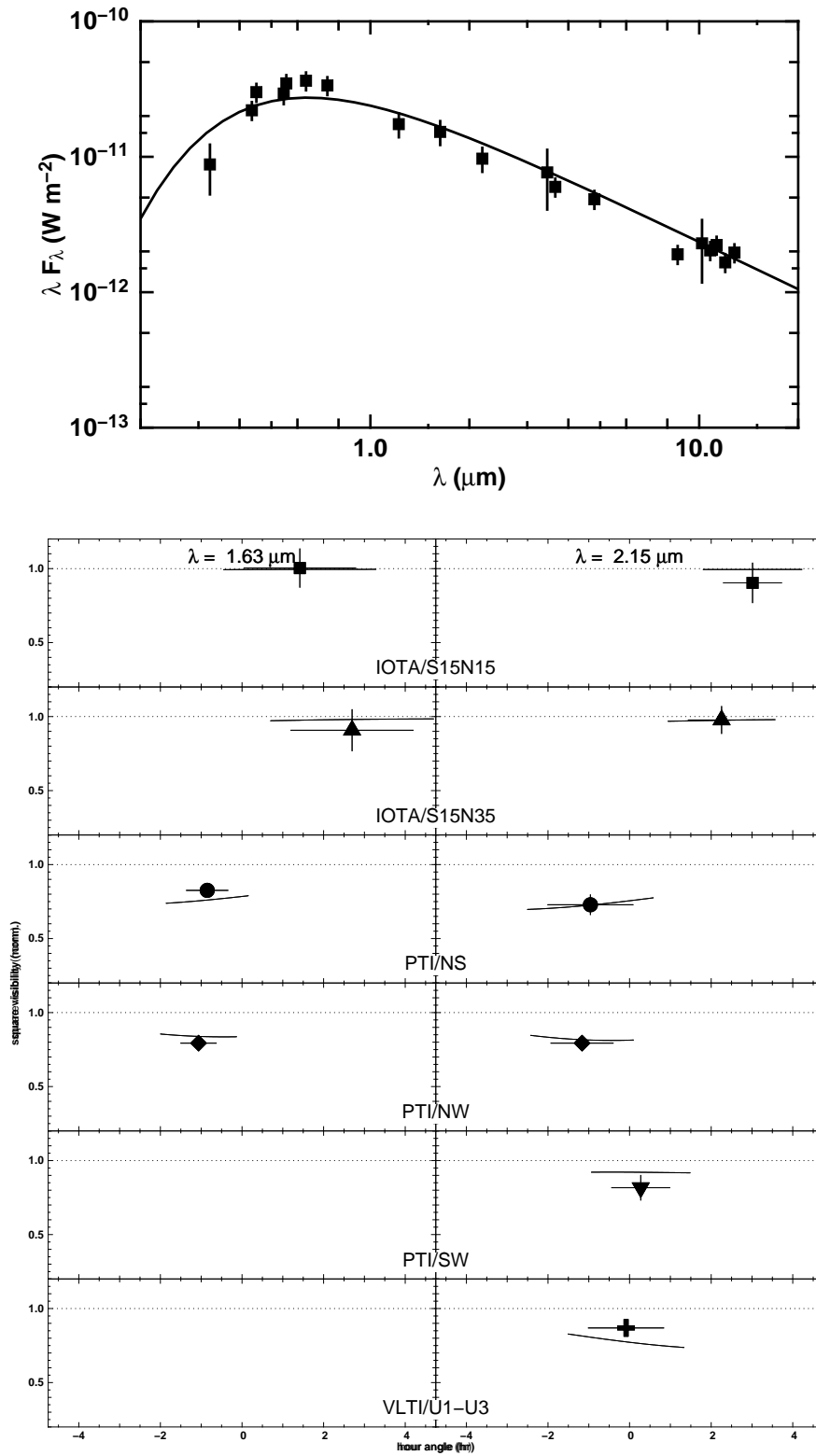


Fig. 7. Data and model for an accretion disk model of FU Ori from Malbet et al. (2005). Top) SED. Bottom) Average visibilities.

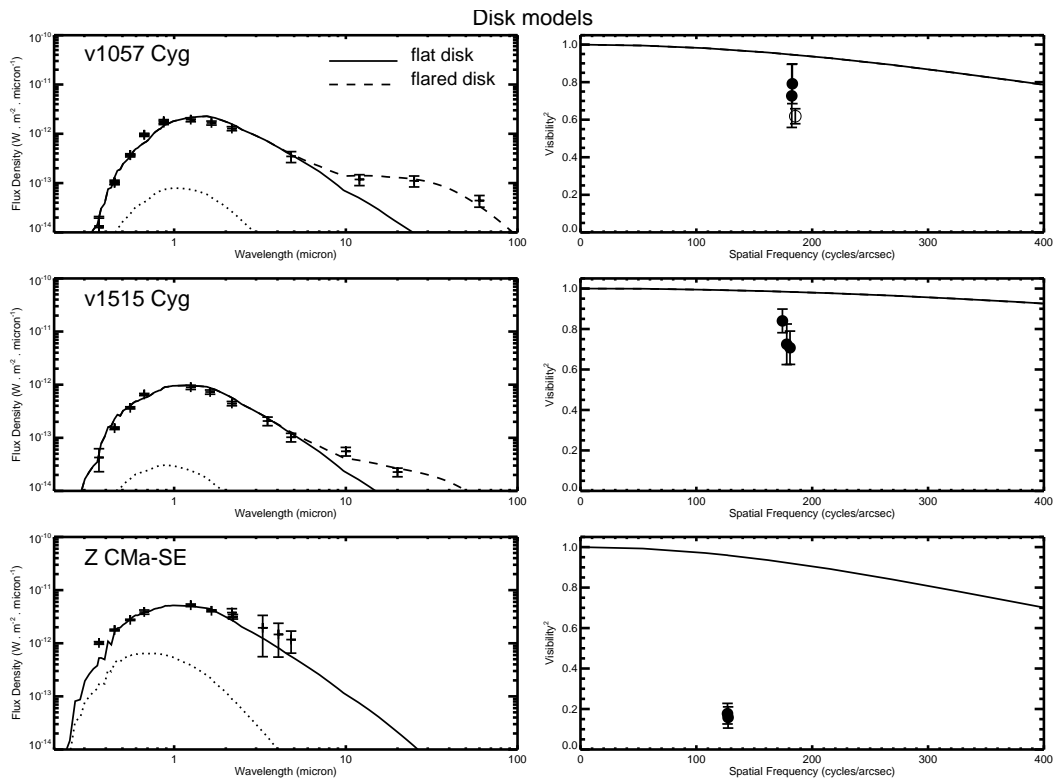


Fig. 8. SEDs and calibrated visibilities for accretion disk models which correspond to best SED fits and are calculated for the parameters of Table 5. The solid line shows the model for a flat disk; the dashed line shows the model for a flared disk. For the flat-disk model, the fitting procedure uses only SED data shortward of $10 \mu\text{m}$, while fitting the flared-disk model uses the whole SED. Figure taken from Millan-Gabet et al. (2006a).

minations with sufficient accuracy to constrain models of pre-main sequence evolution. The first determination of YSO masses with long-baseline interferometry was on the southern binary component of the HD 98800 quadrupole system. Boden et al. (2005) determined the masses with 10% uncertainties and these objects are among the lowest mass ($<0.7 M_{\odot}$) YSOs with dynamically determined masses. Additional systems are being studied (Boden et al., 2007, Schaefer et al, in prep) and will constrain pre-main sequence evolutionary tracks.

6 Debris disks

The list of main sequence stars known to have circumstellar material in the form of debris disks has greatly expanded over the last few years from surveys at longer wavelengths and most recently from Spitzer observations (see the review by Meyer et al., 2007). Given the size and distribution of dust in these disks, it is generally believed that the dust is not remnant from the star

formation process, but rather, is generated through collisions of larger bodies orbiting the star. These disks can extend over 1000 AU from the central star and may be analogs of our own solar system. Many of these systems are only a few hundred million years old and although the material does not have a primordial composition and or distribution, there are many similar aspects in the study of these disks and those around pre-main sequence objects.

Models of material in debris disk systems are a balance of collisions, radiation pressure, Poynting-Robertson drag and the dynamical influence of any large bodies in the system. In order to constrain these models, the dust spatial extent and grain size distribution must be measured. Observations of optical and near-infrared scattered light have provided the most detailed overall picture of the dust distribution. However, these scattered light observations do not have sufficient resolution to characterize the material closest to the star, and this is where infrared interferometry can provide a unique constraint. Spatially resolved observations in the near-infrared provide a much more sensitive probe of the inner regions of these disks. Both PTI (Ciardi et al., 2001) and CHARA (Absil et al., 2006) have detected near-infrared extended emission around Vega, the prototype debris disk system, indicating a 2% excess above the stellar photosphere. While a near-infrared excess was not known through broadband spectral modelling, the interferometrically detected near-infrared excess is within the photometric uncertainties. This technique relies on precise measurement of the visibility (see section 7.2) to measure the departure from the stellar size. An example data set on the debris disk system β Leo is shown in Figure 9. Note that these objects are generally much closer than the nearest YSO's and so the star itself is resolved. The stellar size is determined by the long baseline measurements, and when this is extrapolated to smaller spatial frequencies (shorter baselines), it is clear that the visibility is lower than expected. The data are consistent with an extended (i.e., over-resolved) emission component, which due to the temperatures sampled at 2 microns and the field-of-view, must be at smaller spatial scales than the cooler material which produces the previously known mid-infrared excess toward this star (Akeson et al., in prep).

7 Future prospects

Even as the field of infrared interferometry has greatly expanded in the last several years, current technical developments and new instrumentation will continue this expansion for the next several years. This will allow even more targets to be studied and more detailed studies, in terms of uv coverage and wavelength coverage and resolution of individual objects. Here I discuss a few instrumental improvements which have already been applied to YSO's and are likely to have a big impact in the next few years.

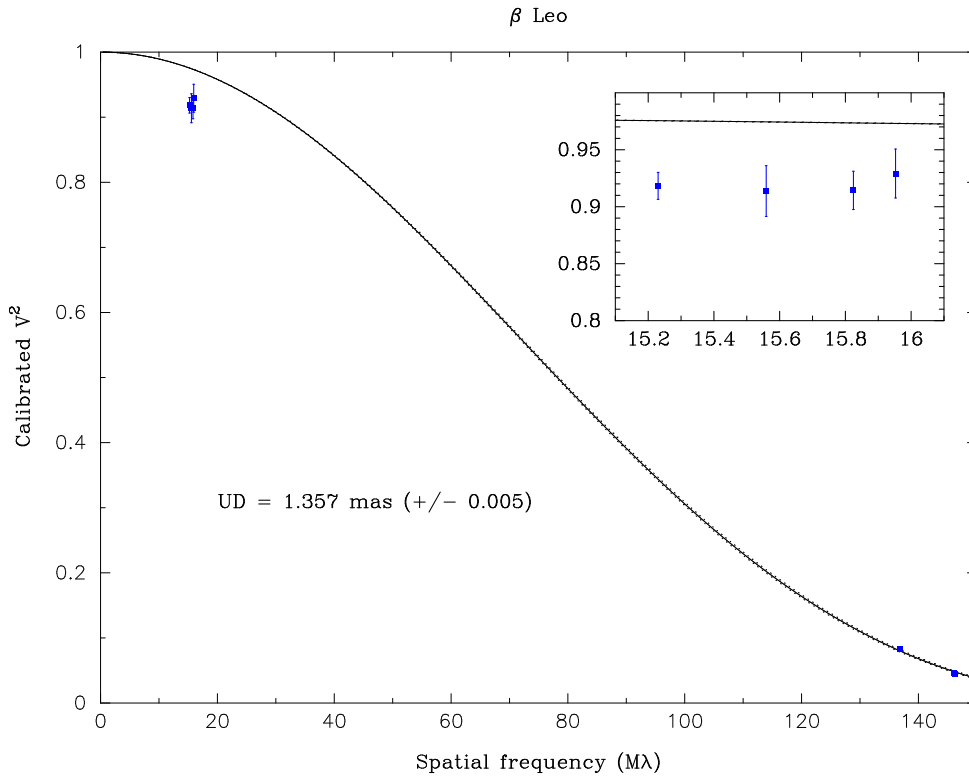


Fig. 9. The measured visibility for β Leo from Akeson et al.(in prep). The higher spatial frequencies are used to constrain the size of the stellar photosphere (which has a uniform disk diameter of 1.357 mas) while the lower than expected visibility on the short baseline indicates the presence of extended emission.

7.1 Better sensitivities

The advent of large aperture interferometers has had the biggest impact in increasing sensitivity, but even these facilities must deal with the realities of interferometry to fully reach their sensitivity limits. The atmosphere and vibrations are major issues and when deciding on observation strategies, you need to balance faster sampling with sensitivity.

One new development which is being actively pursued at KI, VLTI and CHARA is to use dual star and/or phase referencing to increase the sensitivity limit for the target object. This technique uses nearby bright target (or same target at a different wavelength) for tip-tilt/adaptive optics corrections or angle tracking or fringe tracking, thus allowing a longer integration time and better sensitivity limits on the science target.

Improved sensitivity will allow the study of larger range of YSOs. Example classes of objects for which little or no observations have been taken include embedded (Class 1) T Tauris and transition disks. The transition disk stars have a strong excess which starts in mid-infrared, such as TW Hya, and are

often modelled as having a gap or density deficit in the disk. Possible causes of these clearings include photoevaporation and planet formation.

7.2 High dynamic range: precision visibilities

As the disk emission from many very young stellar objects is a significant fraction of the total flux, the resulting visibility is often significantly resolved and in many cases the fringe sensitivity is the driving instrument limitation. However, as YSO's evolve and the disks begin to disperse, the infrared excess decreases and the measured visibility becomes closer to the value for the stellar photosphere alone. At very small disk flux contributions, the precision and accuracy of the visibilities becomes the limiting factor. Many effects need to be controlled or compensated for (see Perrin & Ridgway, 2005, for more details) in order to reach these levels: finite spectral bandwidth, group delay dispersion, finite scan length and differential piston.

Several instruments exist which emphasize precision (including IONIC, FLUOR, VINCI, AMBER) and examples of this data are shown in section 6. High precision visibilities are also very useful in detecting structures within very resolved disks. For example, Malbet et al. (2005) report a small oscillation in the visibility amplitudes for FU Ori which may be due to a bright spot 10 AU from the center of the disk.

7.3 High dynamic range: Nulling

A second technique which is being developed to detect and characterize faint emission is nulling interferometry. In these instruments a destructive fringe is placed on the central source, allowing detection of fainter nearby emission. For example, the KI nuller (Colavita et al., 2006) has been developed to survey nearby main sequence stars for faint emission.

7.4 Closure phase

Closure phase is measured by simultaneously combining the light from 3 or more telescopes and provides information on the target object phase which is uncorrupted by the atmosphere. Even without full aperture synthesis and image reconstruction, closure phase is an important data quantity as it measures skew in the brightness distribution. YSO disks can have significant skew in the case of an inclined disk with a bright inner rim or large flare in which the colder outer material obscures the emission on one side of the central star

but not the other. In the case of the inner rim asymmetry, the closure phase can be used to constrain the geometry. For example, the settling of large dust grain toward the mid-plane will result in a curved rim and therefore lower closure phase (Tannirkulam et al., 2007).

A survey of massive YSOs for closure phase by Monnier et al. (2006) at IOTA found very low closure phases ($<$ several degrees) for most objects. Although the fringe spacings were insufficient to constrain many of the model parameters, the study showed the promise of this technique. An interesting example of detected closure phase in a YSO disk is the observations of AB Aur by Millan-Gabet et al. (2006b). The closure phase was detected on only some of the baselines (Figure 10) and requires an asymmetry in the disk which was not detected in the visibility amplitudes.

7.5 *Imaging*

The next step beyond closure phase is aperture synthesis imaging. Although common in radio interferometry, imaging in infrared interferometry is complicated by the lack of observed baseline visibility phases (which are corrupted by atmospheric noise). However, closure phases can be used in conjunction with visibility amplitudes as the constraints for image reconstruction. Images have been constructed of main-sequence and post-main-sequence stars (Monnier et al., 2007, for example, see the recent image of Altair by), but to date no images have been made of pre-main sequence objects. Several currently operating instruments, including VLT/AMBER and CHARA/MIRC have imaging capabilities and it is merely a matter of time before the first young stellar object images are available.

Imaging is an important step forward for the field of infrared interferometry in general as it reduces the model dependencies in the interpretation of the physical meaning of the data.

8 **Summary**

Star formation is arguably the area of astrophysics in which infrared interferometry has had the biggest impact. The astrophysical highlights of many studies of YSO disks include:

- The optically thick portion of T Tauri and Herbig Ae/Be disks DO NOT extend to a few stellar radii of the stellar surface.

- Emission is coming from near the dust sublimation radius, but not all from a single radius.
- Herbig Ae stars can be either flared or self-shadowed.
- Early Herbig Be stars are consistent with geometrically thin, but optically thick material reaching to within a factor of few stellar radii.
- Grain composition in both Herbig and T Tauri objects indicates radial mixing.

But this has led to a new questions

- What is the exact structure of the dust sublimation boundary?
- How does the inner disk evolve with time?
- How does this effect planet formation and migration?
- Is there an envelope surrounding FU Ori or Herbig stars?
- When do chemical evolution and grain growth start in the disk?

This is an exciting time for the field as observational prospects are rapidly improving. Higher spectral resolution will allow observations of the gas and provide new probes of jets, winds, and accretion onto the central star. Closure phase and imaging will help eliminate model uncertainties and dependencies.

Thanks to R. Millan-Gabet and F. Malbet for providing material both for the talk and for the proceedings. Thanks to E. Tatulli and S. Kraus for providing figures.

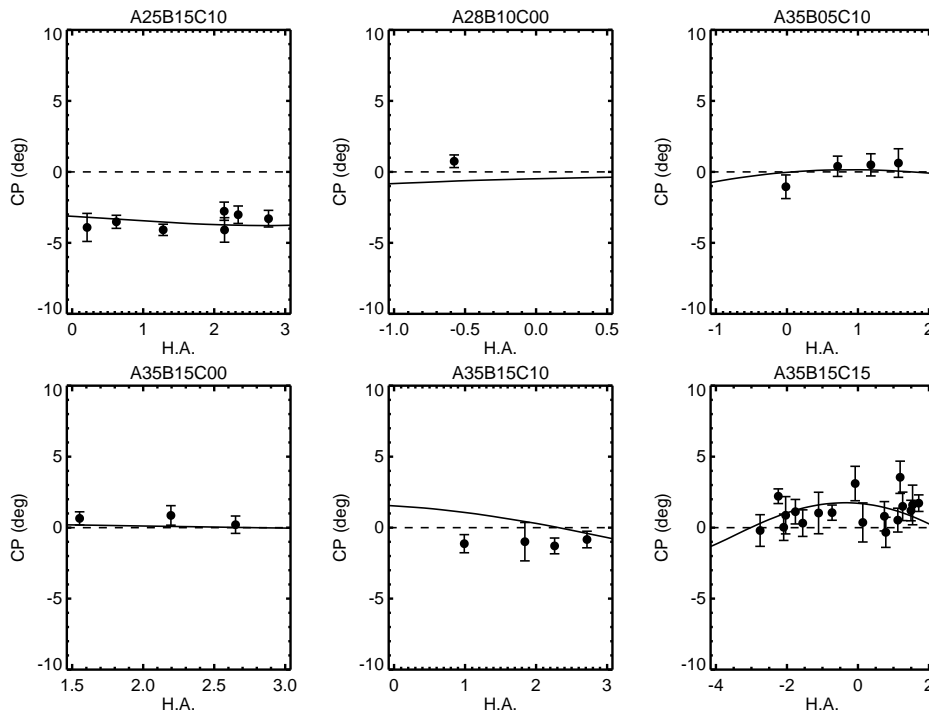
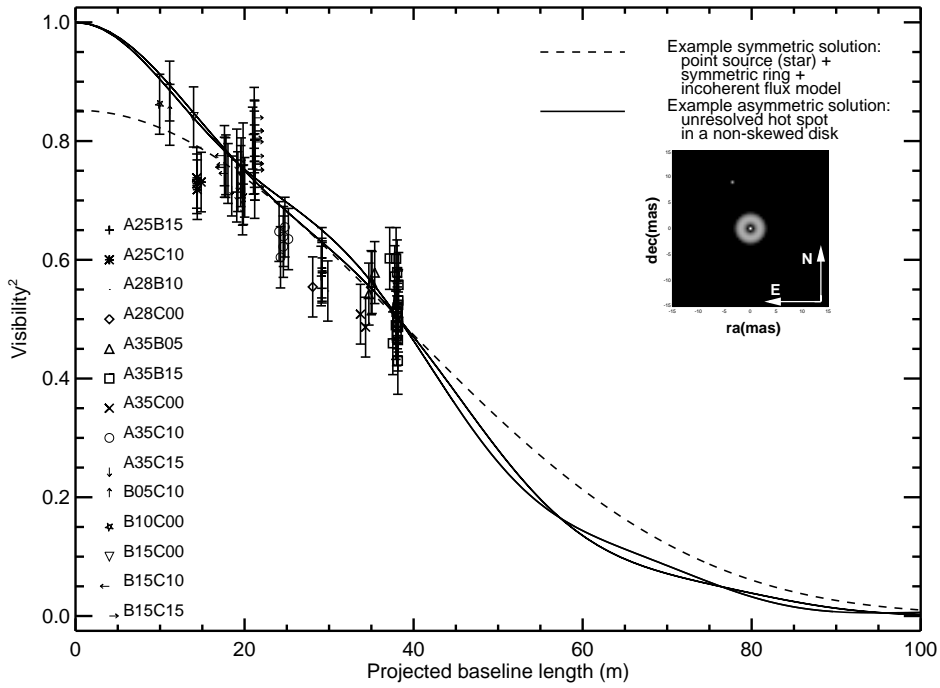


Fig. 10. Top) Calibrated visibility data as a function of projected baseline length, and comparison to the two models discussed in the text. For the asymmetric model, the plot shows cuts in the (u, v) -plane along two distinct directions that encompass most of the AB Aur data. Bottom) Calibrated closure phase as a function of hour angle for AB Aur. Taken from Millan-Gabet et al. (2006b)

References

- Ábrahám P., Mosoni L., Henning Th., Kóspál Á., Leinert Ch. et al., 2006, *A&A*, 449, L13
- Absil O., di Folco E., Mérand A., Augerau J.-C., Coudé du Foresto V. et al., 2006, *A&A*, 452, 1, 237, 244.
- Akeson R. L., Ciardi D. R., van Belle G. T., Creech-Eakman M. J., and Lada E. A., 2000, *ApJ*, 543, 313.
- Akeson R. L., Boden A. F., Monnier J. D., Millan-Gabet R., Beichman C. et al., 2005, *ApJ*, 635, 1173
- Akeson R. L., Walker C. H., Wood K., Eisner J. A., and Scire E., 2005, *ApJ*, 622, 440
- Beuther, H., Churchwell, E. B., McKee, C. F., & Tan, J. C. 2007, *Protostars and Planets V*, 165
- Bockelée-Morvan, D., Gautier, D., Hersant, F., Huré, J.-M., and Robert, F. 2002, *A&A*, 384, 1107
- Boden, A. F., et al. 2005, *ApJ*, 635, 442
- Boden, A. F., et al. 2007, *ApJ*, in press
- Ciardi D. R., van Belle G. T., Akeson R. L., Thompson, R. R., Lada, E. A., 2001, *ApJ*, 559, 1147
- Colavita, M. M., Serabyn, G., Wizinowich, P. L., & Akeson, R. L. 2006, *Proc. SPIE*, 6268
- Dominik, C., Dullemond, C. P., Waters, L. B. F. M., & Walch, S. 2003, *A&A*, 398, 607
- Dullemond C. P., Dominik C., and Natta A. 2001, *ApJ*, 560, 957
- Eisner J. A., Lane B. F., Hillenbrand L. A., Akeson R. L., and Sargent A. I. 2004, *ApJ*, 613, 1049
- Eisner J. A., Hillenbrand L. A., White R. J., Akeson R. L., and Sargent A. I. 2005, *ApJ*, 623, 952.
- Eisner J. A., Chiang, E. I., and Hillenbrand, L. A. 2006, *ApJ*, 637, L133
- Gail H.-P. 2004, *A&A*, 413, 571
- Hartmann L. and Kenyon S. J. 1996, *Ann. Rev. Astron. Astrophys.*, 34, 207
- Klein, R. I., Inutsuka, S.-I., Padoan, P., & Tomisaka, K. 2007, *Protostars and Planets V*, 99
- Leinert Ch., et al. 2004, *A&A*, 423, 537
- Malbet F., et al. 1998, *ApJ*, 507, L149
- Malbet F., et al. 2005, *A&A*, 437, 627
- Malbet, F., et al. 2007, *A&A*, 464, 43
- Meeus G., et al. 2001, *A&A*, 365, 476-490.
- Meyer, M. R., Backman, D. E., Weinberger, A. J., & Wyatt, M. C. 2007, *Protostars and Planets V*, 573
- Millan-Gabet R., Schloerb F. P., Traub W. A., Malbet F., Berger J.-P., and Bregman, J. D. 1999, *ApJ*, 513, L131-L143.
- Millan-Gabet R., Schloerb F. P., and Traub W. A. 2001, *ApJ*, 546, 358-381.
- Millan-Gabet R., et al. 2006, *ApJ*, 641, 547-555.

- Millan-Gabet R., Monnier J. D., Berger J.-P., Traub W. A., Schloerb F. P. et al. 2006, *ApJ*, 645, 1, L77
- Millan-Gabet, R., Malbet, F., Akeson, R., Leinert, C., Monnier, J., & Waters, R. 2007, *Protostars and Planets V*, 539
- Monnier J. D. and Millan-Gabet R. 2002, *ApJ*, 579, 694-698.
- Monnier J. D., et al. 2005, *ApJ*, 624, 832-840.
- Monnier J. D., et al. 2006, *ApJ*, 647, 444
- Monnier, J. D., et al. 2007, *Science*, 317, 342
- Muzerolle, J., Calvet, N., Hartmann, L., & D'Alessio, P. 2003, *ApJL*, 597, L149
- Natta A., Prusti T., Neri R., Wooden D., Grinin V. P. et al. 2001, *A&A*, 371, 186-197.
- Perrin, G., & Ridgway, S. T. 2005, *ApJ*, 626, 1138
- Preibisch, T., Kraus, S., Driebe, T., van Boekel, R., & Weigelt, G. 2006, *A&A*, 458, 235
- Quanz, S. P., Henning, T., Bouwman, J., Ratzka, T., & Leinert, C. 2006, *ApJ*, 648, 472
- Tannirkulam, A., Harries, T. J., & Monnier, J. D. 2007, *ApJ*, 661, 374
- Tatulli, E., et al. 2007, *A&A*, 464, 55
- Tuthill, P. G., Monnier, J. D., Danchi, W. C., Hale, D. D. S., & Townes, C. H. 2002, *ApJ*, 577, 826
- van Boekel R., et al., 2004, *Nature*, 432, 479